# A First Principles Study on the Structure of Ice-VI: Static Distortion, Molecular Geometry, and Proton Ordering†

**Jer-Lai Kuo*,‡ and Werner F. Kuhs*,§**

*School of Physical and Mathematical Sciences, Nanyang Technological University, 1 Nanyang Walk, Singapore 637616, Singapore, and GZG Crystallography, Universität Göttingen, Goldschmidtstrasse 1, 37077 Göttingen, Germany*

*Received: September 16, 2005; In Final Form: January 12, 2006*

We have studied the structure of ice-VI by examining all ice-rule-allowed structures in its primary unit cell of 10 water molecules with first principles methods. A significant amount of static distortions in the oxygen positions away from their crystallographic positions are found, which is in good agreements with significant higher-order terms in the atomic displacement parameters obtained from X-ray and neutron diffraction data. Structural anomalies (such as exceptionally short OH bonds and small H−O−H angles) noted in conventional crystal structure refinements were not seen in our ab initio calculations, and it is evident that these structural anomalies arose from oversimplified models in which static distortions are not properly accounted for. Our results also show that the molecular geometry of water in ice-VI is similar to but richer than those in ice-Ih and ice-VII. Larger distortions in bond lengths/angles and correlation between the molecular geometry and the neighboring environments were found. Different proton-ordering schemes proposed in the literature were examined, and our calculations provide evidence in favor of a ferroelectric phase of the proton-ordered counterpart of ice-VI at about 80 K.

## I. Introduction

Ice-VI plays a key role in connecting our understanding of the structures of various phases of ice that compose the rich and complicated phase diagram of water.[1,2] Similar to other high-pressure phases (ice-VII, ice-VIII, and ice-X), there are two interpenetrating but independent hydrogen-bonded (H-bonded) sublattices in ice-VI. However, the molecular geometry of water molecules in ice-VI is closely related to other intermediate pressure phases (ice-II, ice-III, ice-IV, ice-V, and ice-IX), which are characterized by considerable distortions in bond angles and distances. In fact, ice-VI shows the largest H-bond bending of all known phases of ice, twice as large as those in ices II and III and 50% larger than that in ice-V. Neutron diffraction data suggested that the H−O−H angles in ice-VI vary between 98.0° and 115.5° in contrast to that in ice-VII where the distribution centers at 105.6° with a small variation.[3]

Ice-VI occupies a unique position in the phase diagram of $H_2O$; for example, ice-VI has four triple points (of which three are experimentally well established), and there could potentially be two more triple points if the existence of a low-temperature proton-ordered counterpart of ice-VI is confirmed. In comparison to ice-V and all lower-pressure forms of ice, the denser packing of ice-VI (1.373 g/cm$^3$ at 225 K and 1 GPa) is achieved by interpenetration of two independent H-bonded networks. The density is comparable to that of high-density amorphous (HDA) ice as well as the recently discovered very-high-density amorphous (VHDA) ice at correspondingly higher pressures.[4−7] In fact, the formation conditions for both HDA and VHDA are within the stability region of ice-VI. Partly overlapping with the stability field of ice-VI is also the field of existence of metastable ice-XII,[8] which consists of noninterpenetrating seven- and eight-membered rings producing similar molecular densities as ice-VI. While it was suggested earlier that HDA and VHDA may contain self-interpenetrating H-bonded networks,[9] recent work indicates that such networks are not present; neutron spectroscopy[6] does not find evidence for features related to interpenetrating lattices and molecular dynamics simulations[10] suggest that the density increase compared to the low-density amorphous (LDA) form is achieved by building ring structures larger than six-membered and shifting the predominant size with increasing pressure.[11] Therefore, it seems that the interpenetrating networks of ice-VI, the thermodynamically stable form of condensed water in the pressure range from 0.6 to 2 GPa, presents a rather unique structure not easily reproduced locally in low-temperature preparations of the amorphous forms in this pressure range.

The crystal structure of ice-VI was first determined by Kamb[12] in 1965 on samples recovered to ambient pressure at 98 K. The space group of $P4_2/nmc$ and a tetragonal unit cell consisting of 10 water molecules were assigned. The first direct measurement of the structure of ice-VI under pressure was carried out by Kuhs et al.[3] in 1984 using powder neutron diffraction. More accurate X-ray and neutron diffraction measurements were subsequently carried out by Kuhs and coworkers.[13−16] Significant higher-order terms in the structural analysis were found, and the authors attributed the origin of the high-order terms to the existence of static displacement of oxygen atoms from their high-symmetry crystallographic positions.[17]

Static distortions away from the high-symmetry sites are common in various "crystalline" phases of ice as the orientations of water molecules are random, and therefore individual molecules can deviate from their lattice sites and change their

† Part of the special issue "Michael L. Klein Festschrift".

* Authors to whom correspondence should be addressed. E-mail: jlkuo@ntu.edu.sg; wkuhs1@gwdg.de.

‡ Nanyang Technological University.

§ Universität Göttingen.

10.1021/jp055260n CCC: $33.50 
Published on Web 02/01/2006

molecular angles and bond lengths in response to different arrangements of the neighboring molecules. In contrast to phases of higher symmetry (for example, ice-Ih[18] and ice-VII[3]) on which various elaborate disorder models were tested for crystal structure refinement, the more difficult detailed crystallographic analysis for the oxygen displacements from positions of lower symmetry have not yet been performed. Hence, one of our objectives in this work is to use first principles calculations to assess the amount of static distortions as well as to study how water molecules adjust their molecular geometries to different environments.

The H-bond orientation in ice-VI is found to be random,[12] and two possible schemes for a low-temperature proton-ordered phases were proposed by Kamb[19] (recovered samples, antiferroeletric ordering) and Johari and Whalley (under-pressure, ferroelectric ordering).[20,21] However, neither scheme has support from neutron in situ diffraction measurements.[3] It is important to keep in mind that a significant difference in lattice constants was found in recovered and under-pressure samples. Thus, to test the possible ordering scheme of either type, we also need to take into account the possible effects of the lattice constants; proton-ordering and lattice constants were found to be interrelated in the case of ice-III/IX.[22] Although the energy difference between the order and the disorder configurations is small (so is the low phase transition temperature), the applicability of our methodology has been validated by its success in describing the correct ground-state (proton-ordered) structures for ice-VII[23,24] and ice-Ih.[24,25] It is worth mentioning that the most reputable empirical force fields failed to reproduce the latter.[26]

The remainder of this paper is structured as follows. In section 2, we will summarize the structure of ice-VI and briefly cover the enumeration of all ice-rule-allowed configurations in its primary unit cell as well as the procedure to generate their initial geometries. We will also provide a detailed description of our geometry optimization procedure and issues regarding *k*-point sampling and the lattice constants. In section 3, we will present the relative energetics and structural data of all 45 ice configurations predicted by ab initio calculations and compare them with experimental results. We shall conclude with a short summary.

## 2. Methodologies

**Generation of Ice-Rule-Allowed Configurations.** The symmetry group of ice-VI is $P4_2/nmc$, which requires a proton-disordered structure. The primary unit of ice-VI (shown in Figure 1) is a tetragonal cell with 10 water molecules, and among them there are two kinds of crystallographically distinct oxygen atoms with multiplicities of 2 and 8. From the convention used in previous neutron diffraction studies,[3,13,16] the former is denoted as $O_1$ and the latter $O_2$ (their positions are shown with different colors in Figure 1A). Similar to other high-pressure phases of ice, ice-VI has two interpenetrating and independent sublattices shown by the color-coding scheme shown in Figure 1B. One can also describe each of the sublattices as a network of connected water hexamer cages (Figure 2).

The orientation of the water molecules in ice-VI is found to be random and assumed to be subjected only to the constraints of the ice rules.[27,28] As a first step to understand the effects of H-bond orientation on the structure of ice-VI, we enumerated all the possible configurations in the primary unit cell. We found 576 possible arrangements of the H-bond network satisfying ice rules, and most of these configurations are chemically identical, meaning that they are related by some symmetry operations. For all "chemically identical" structures, only one representative is needed for further detailed examinations. The elimination of symmetrical-related configurations can be quickly done by employing the graph invariance algorithm[29] that has been detailed in previous works,[23,25,30] and we found that there are only 45 symmetrically distinct configurations.

To generate the structure of these 45 configurations, we need to assign the initial coordinates for the oxygen and hydrogen atoms. For the oxygen atoms, we use the experimental positional

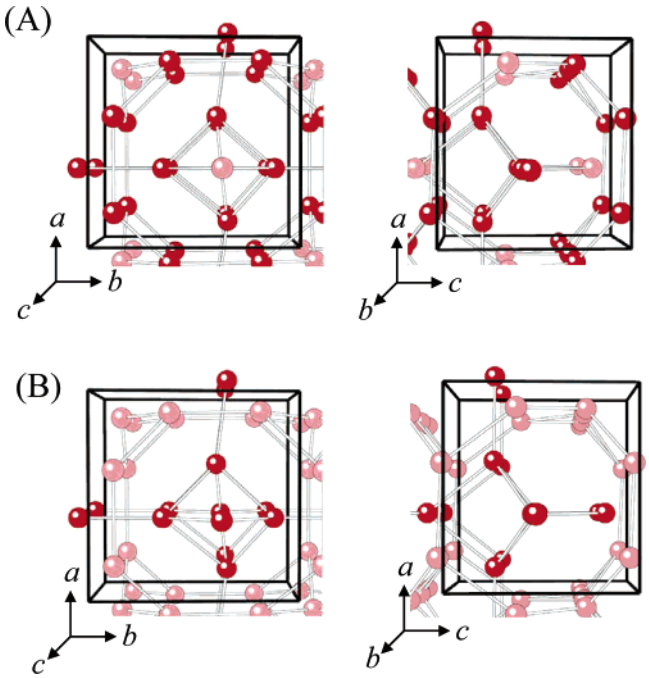


**Figure 1.** Structure of the oxygen lattice of ice-VI in its primary unit cell. In the two upper figures (Figure 1A), two kinds of crystallographically distinct oxygen atoms are color-coded differently. The primary unit cell has tetragonal symmetry, and there are 10 water molecules. The multiplicity of $O_1$(pink) and $O_2$(red) are 2 and 8, respectively. Similar to other high-pressure phases of ice, ice-VI has two interpenetrating and independent sublattices, and we highlighted the two sublattices with different colors in the two lower figures (Figure 1B). Focusing on the red sublattice in the lower-right figure, it is easy to see that each of the sublattices can be regarded as a network of water hexamer cages (as shown in Figures 2 and 3).

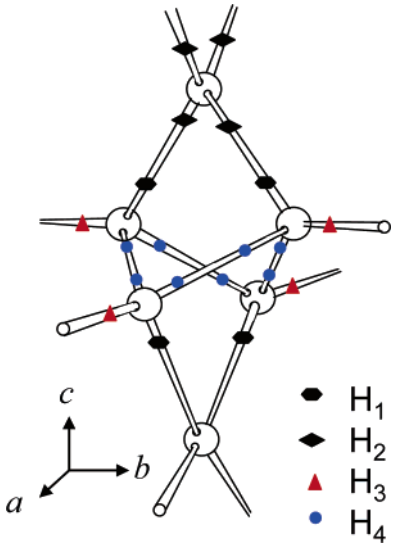


**Figure 2.** The four kinds of crystalgraphically distinct hydrogen positions in ice-VI. In other words, there are four kinds of H-bonds. The averaged structural data of the H-bonds are summarized in Table 2.

parameters from neutron diffraction data.[3] For simplicity, the initial positions of the hydrogen atoms are assigned to locate along the straight line between two oxygen atoms, and the initial oxygen−hydrogen bond length is assumed to be one-third of the oxygen−oxygen distance.

Special attention was paid to test the influence of lattice constants on the structure and the relative energies of different ice configurations. It is important to note in this context that (1) experimental measurements on under-pressure[3] and recovered samples[12] showed significant difference in the lattice constants and (2) different proton-ordering schemes were proposed by Kamb (recovered samples, antiferroelectric)[19] and Johari and Whalley (under-pressure, ferroelectric).[21] In total, three sets of lattice constants were used (1) $a = 6.27$ Å, $c = 5.79$ Å (recovered samples),[12] (2) $a = 6.166$ Å, $c = 5.689$ Å (1.1 GPa and 8 K)[3], and (3) $a = 6.181$ Å, $c = 5.698$ Å (1.1 GPa and 225 K)[3].

**Geometry Optimization.** In the geometry optimization all degrees of freedom are allowed to relax, except the lattice constants. All ab initio calculations are carried out using the Car−Parrinello molecular dynamics methods (CPMD)[31] based on the Becke−Lee−Yang−Parr (BLYP)[32,33] functional, using norm-conserving pseudo-potentials (Troullier and Martins form)[34] with a plane-wave cutoff of 70 Ry, and considering only the Γ point of the Brillouin zone. These are the standard conditions employed in numerous investigations of liquid water[35−37] and crystalline phases of ice.[23,24,25]

There are some concerns in the literature about the *k*-point sampling (that is sufficient *k*-point sampling is required to achieve convergence of the total energy). In our previous study on ice-VII and ice-VIII,[23,24] we found that while the total energy converges slowly with respect to the *k*-point used, the molecular geometry is not sensitive to the increase in *k*-point mesh. Hence all geometry optimizations were carried out with the Γ point only, and total energy from single-point calculations with a $2 \times 2 \times 2$ mesh (Monkhorst−Pack scheme) were used to calculate the relative stability.

## 3. Results and Discussions

**Static Distortion of the Oxygen Lattice.** In principle the amount of static distortion can be extracted either from the temperature dependency of atomic displacement parameters, from their higher-order terms, or from introducing suitable split position models.[17] This has been done on various phases of ice with high symmetry.[3,38,39] The relatively low local symmetry of the oxygen positions in ice-VI leads to a large number of degrees of freedom for split models, and it is very difficult to obtain reliable structural refinements with so many free parameters. However, single-crystal data have permitted determination of atomic displacement parameters up to fourth order,[7] often indicative of static displacements, but more difficult to evaluate quantitatively.[9] Theoretical calculations, however, can offer detailed structural insights and give a quantitative description on the amount of static distortion.

There are two major categories of static distortions. First, we consider the amount of deviation for an oxygen atom from its averaged crystallographic position (denoted as $\delta$). This kind of distortion is very common in most phases of crystalline ice, and the tetragonal symmetry of ice-VI gives two distinct directions; therefore the amount of $\delta$ in $O_1$ can be separated in $\langle 100 \rangle$ ($\delta^1_{ab}$) and $\langle 001 \rangle$ ($\delta^1_c$). Another kind of distortion arises from the fact that ice-VI has two independent sublattices. We use $\epsilon$ to represent the amount of relative deviation of the two sublattices compared to is experimental averaged structure. Similarly, the amount of $\epsilon$ in $\langle 100 \rangle$ and $\langle 001 \rangle$ are represented by $\epsilon_{ab}$ and $\epsilon_c$, respectively.

**TABLE 1: Comparison on the Static Distortion in Ice-VI, Ice-VII,[23] and Ice-Ih[25] from First Principles Calculations[a]**

| | ice-VI | ice-VII | ice-Ih |
|---|---|---|---|
| $\langle\epsilon\rangle$ | $\langle\epsilon_{VI}\rangle \approx 0.045$ ($\langle\epsilon_{ab}\rangle \approx 0.037$, $\langle\epsilon_c\rangle \approx 0.026$) | $\langle\epsilon_{VII}\rangle \approx 0.051$ | N/A |
| $\langle\delta^1\rangle$ | $\langle\delta^1{}_{VI}\rangle \approx 0.040$ ($\langle\delta^1{}_{ab}\rangle \approx 0.037$, $\langle\delta^1{}_c\rangle \approx 0.014$) | $\langle\delta_{VII}\rangle \approx 0.060$ | $\langle\delta_{Ih}\rangle \approx 0.047$ |
| $\langle\delta^2\rangle$ | $\langle\delta^2{}_{VI}\rangle \approx 0.043$ ($\langle\delta^2{}_{ab}\rangle \approx 0.027$, $\langle\delta^2{}_c\rangle \approx 0.033$) | | |

[a] The units are in angstroms, and the tetragonal symmetry of ice-VI gives two distinct directions: *ab* stands for $\langle 100 \rangle$ and *c* for $\langle 001 \rangle$. The isotropic averages in ice-VI are comparable to the amount of static deviations in ice-VII and ice-Ih and also in reasonable agreement with indirect experimental estimates (see the text for details).

Our theoretical estimate on the different sources of static distortion is summarized in Table 1. The isotropic averages are $\langle\delta^1\rangle = 0.040$ Å, $\langle\delta^2\rangle = 0.043$ Å, and $\langle\epsilon\rangle = 0.045$ Å; these numbers are comparable with their counterparts in ice-VII ($\langle\epsilon^{VII}\rangle \approx 0.051$ Å and $\langle\delta^{VII}\rangle \approx 0.060$ Å)[23] and ice-Ih ($\langle\delta^{Ih}\rangle \approx 0.047$ Å)[25] assessed via first principles calculations. We should point out that the above-mentioned averages only reflect the overall static distortions, and individual ice configurations could show large deviations. For example, the structure depicted in Figure 5 bears large $\epsilon_{ab}$ and very small $\epsilon_c$, and there are many other structures showing the counteracting trends. Nevertheless, it is interesting to note that unlike the case of ice-VII in which there exists a clear correlation between the relative stability of a ice configuration and its $\epsilon$ (Figure 4 in ref 23), no simple correlation between the energetics with either $\epsilon$ or $\delta$ is found in ice-VI. A systematic study of connecting the energetics of an ice configuration with its H-bond topology patterns can be done by employing graph invariant methods[29,30] and shall be addressed in a future publication.

**Molecular Geometry of $H_2O$ and H-Bonding.** The fact that each of the sublattices in ice-VI can be viewed as a network of cage water hexamers provides interesting comparisons. First, for the isolated water hexamers (there are 27 symmetrically distinct isomers),[40] different ab initio methods can be applied to assess the accuracy of density functional theory (DFT)/generalized gradient approximation (GGA) used herein. Second, by comparing the water structure in hexamers and in ice-VI, we can also separate the influence due to local constraints from the effects due to periodic boundary conditions.

The four crystallgraphically distinct hydrogen positions in ice-VI are shown in Figure 2. In other words, there are four kinds of H-bonds, and in this work we adapted the notations used in previous neutron diffraction experiments.[3] $H_2$ atoms are the only species that is covalently bonded to $O_1$, and $H_1$ atoms are the complementary half-hydrogen positions of $H_2$ along the same H-bond. $H_3$ are those sitting on the H-bonds that connect the water hexamers in the *a* and *b* directions. $H_4$ are hydrogen positions on the puckered four-membered H-bonded rings (oriented perpendicular to the *c*-axis) of the hexamer units

The averaged structural data of the different H-bonds from our ab initio calculations are summarized in Table 2. For comparison, we also listed the results from previous neutron diffraction experiments.[3] In general, the ab initio calculations agree well with the experimental data except for the *R*(OH) length. The surprisingly short *R*(OH) length ($<0.94$ Å) resulting from a standard crystallographic analysis of the neutron diffraction data is likely due to the neglect of static distortions in the oxygen lattice; we will elaborate on this below. It is well-

**TABLE 2: Averaged Molecular Geometry of Water in Ice-VI Determined by Neutron Diffraction[3], DFT Calculations in Ice-VI, and DFT Calculations in $(H_2O)_6$ Cages[a]**

| | multiplicity | $R_{OO}$ | ∠OHO | $R_{OH}$ | $R_{OO}$ | ∠OHO | $R_{OH}$ |
|---|---|---|---|---|---|---|---|
| $O_2-H_1\cdots O_1$ | 8 | *2.788(24)* | *161.81(5.19)* | *0.937(55)* | **2.8141(189)** | **161.18(2.49)** | **0.9912(12)** |
| $O_1-H_2\cdots O_2$ | 8 | *2.788(24)* | *161.58(4.41)* | *0.986(48)* | **2.8036(262)** | **161.40(1.36)** | **0.9921(10)** |
| $O_2-H_3-O_2$ | 8 | *2.726(38)* | *175.22(4.33)* | *0.976(51)* | **2.8148(104)** | **176.51(2.04)** | **0.9884(07)** |
| $O_2-H_4-O_2$ | 16 | *2.778(28)* | *156.64(3.09)* | *0.939(32)* | **2.8001(226)** | **158.16(2.10)** | **0.9909(13)** |

| | multiplicity | ∠H−O−H | ∠O−O−O | ∠H−O−H | ∠O−O−O | ∠H−O−H | ∠O−O−O | Figure 3 |
|---|---|---|---|---|---|---|---|---|
| $\angle H_2-O_1-H_2$ | 1 | *97.97(4.77)* | *76.61(73)* | **101.71(29)** | **76.07(16)** | ***103.09(42)*** | ***72.67(99)*** | A |
| | 2 | *115.51(2.29)* | *128.02(45)* | **107.35(12)** | **125.03(53)** | ***106.33(34)*** | | B |
| $\angle H_4-O_2-H_4$ | 2 | *101.29(3.40)* | *76.90(92)* | **101.80(19)** | **75.90(20)** | ***102.94(39)*** | ***73.93(1.53)*** | C |
| $\angle H_1-O_2-H_4$ | 4 | *105.67(3.40)* | *89.32(78)* | **103.51(19)** | **89.57(1.44)** | ***103.88(39)*** | ***90.46(3.41)*** | D |
| $\angle H_1-O_2-H_3$ | 2 | *113.07(4.86)* | *128.30(96)* | **108.08(18)** | **125.65(63)** | ***106.34(1.32)*** | | E |
| $\angle H_3-O_2-H_4$ | 4 | *114.97(2.92)* | *128.45(75)* | **107.66(19)** | **123.97(80)** | ***106.62(1.00)*** | | F |

[a] Neutron diffraction (italic text), DFT calculations in ice-VI (bold text), and DFT calculations in $(H_2O)_6$ cages (bold italic text). Bond lengths are in angstroms, and bond angles are in degrees. The standard deviations are given in brackets.

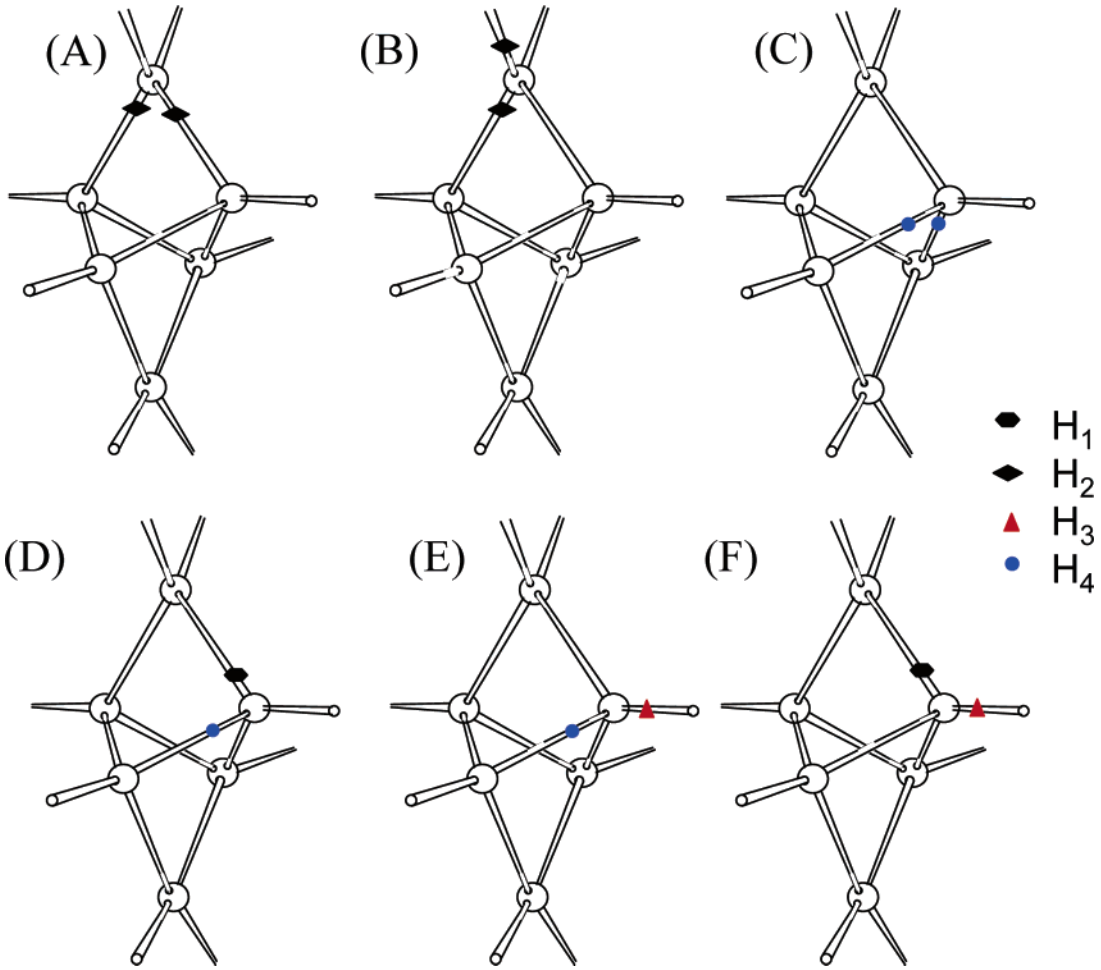


**Figure 3.** Six distinct orientations of a water molecule in ice-VI. Parts A and B are centered at $O_1$, and parts C, D, E, and F are centered at $O_2$. Their averaged molecular geometry and multiplicity are detailed in Table 2. The general trends are (1) water molecule orientations in a four-membered ring (such as those in parts A, C, and D) have smaller H−O−H angles and (2) water molecule orientations in an eight-membered ring (such as those in parts B, E, and F) have larger H−O−H angles.

known that DFT/GGA methods tends to overestimate the *R*(OH) length.[41] In our previous studies we found that the amount of elongation in *R*(OH) length is about 0.01 Å in both ice-Ih[25] and ice-VII.[23] Assuming the elongation of the *R*(OH) length is similar here, the averaged *R*(OH) in ice-VI is about 0.98 Å. This estimate agrees with the experimental estimate based on the empirical relation between the OH distance and stretching frequency,[42] and it is also similar to the *R*(OH) length in the water hexamers.[40]

The six symmetrically distinct orientations of water are shown in Figure 3. For water molecules centered at $O_1$, there are two distinct orientations (shown in Figures 3A and 3B). Orientation A is part of a four-membered ring, and in orientation B the shortest loop consists of eight water molecules on several hexamer units. Similarly, the four symmetrically distinct orientations for $H_2O$ centered at $O_2$ can be organized as the following: Orientations C and D are part of the four-membered ring, and D and E belong to an eight-membered ring. In short,

the shortest H-bond loops in ice-VI are either four- or eight-membered (as opposed to a homogeneous size of six in ice-Ih and ice-VII), and it is worth mentioning that these loop sizes are among the smallest and largest found in the crystalline phases of ice.

While the variation in $R$(OH) is small in ice-VI, the molecular angle of water ($\angle$HOH) appears to be more sensitive to the molecular orientations (summarized in Table 2). It is not surprising that the $\angle$HOH would be strongly affected by the $\angle$OOO to accommodate a reasonable H-bonding angle. Nevertheless it is clearly indicated in Table 2 that even under extreme cases (where $\angle$OOO is less than 90°) the molecular angle remains much closer to its gas-phase value than previous interpretations based on neutron diffraction data.[3] Our ab intio calculations indicate the small $\angle$HOH angles (i.e., parts A, C, and D in Figure 3) in ice-VI range from 101.71° to 103.51°. It is intriguing to note that while the $\angle$OOO angles in ice-VI are larger than their counterparts in water hexamers, the $\angle$HOH angles show the opposite trend. We think the reduction in $\angle$HOH is mostly likely due to the repulsive force between water molecules in the independent sublattices, and our conjecture is supported by the observation that the molecular angle in ice-VII[23] is 105.38(26)°as compared to the molecule angle of 106.34(36)°in ice-Ih.[25]

It is fairly clear from the above discussions that the molecular geometry of water in ice-VI remains normal as compared to its gas-phase value and structural anomalies (such as very short $R$(OH) and improbable $\angle$HOH ) indicated in conventional structural refinements[3] can be attributed to the fact that an oversimplified model (that cannot appropriately consider all sorts of static distortions caused by the randomness of the H-bond orientation) were used for structure refinement.

**Proton Ordering.** *Possible Low-Temperature Proton-Ordered Phase and the Effect of Lattice Constants.* There are indirect evidences for proton ordering in ice-VI, but the low-temperature proton-ordered form has not been identified by direct neutron diffraction experiments. In fact, two possible proton-ordering schemes were proposed by Kamb (recovered samples, antiferroelectric)[19] and Johari and Whalley (under-pressure sample, ferroelectric).[21] Furthermore, Kuhs et al.[12] pointed out the significant difference in lattice constants between under-pressure[3] and samples recovered to ambient pressure.[12] This raises concerns on the possible interrelation of the lattice constants with the actual proton ordering.

The energies of all 45 symmetrically distinct ice configurations of ice-VI are shown in Figure 4, where the zero of the energy scale is set to the averaged energy. In light of the possible effects of different lattice constants in recovered and under-pressure samples, we have reoptimized all 45 ice configurations under several sets of lattice constants under different experimental conditions (details see the caption of Figure 4). It is evident from Figure 4 that lattice constants play a very minor role in the relative stabilities, and under all three sets of lattice constants we considered, a ferroelectric structure shown in Figure 5 is found to be the ground-state configuration.

Furthermore, the energy "gap" between the most stable and the second most stable configurations is about 0.5 mhartree, regardless of the lattice constants used. Although the relative stabilities of a few configurations in the intermediate range are altered, it would not affect the results discussed herein. As a rough estimate, we can calculate the "thermal properties" using the following approximated partition function, $Q_N = \Sigma_i^M f_i \exp(-\beta E_i)$, where $E_i$ is potential energy of the $i$th configuration, $f_i$ is the number of symmetry-related configurations that are represented by $i$th configuration, and $M$ is the total number of symmetrically distinct representatives.[23,29]

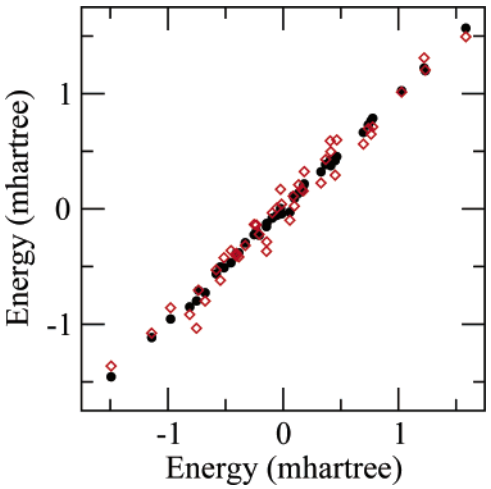


**Figure 4.** Effects of lattice constants on the relative energetics. The $x$-axis is the energy difference (in mhartree) of all 45 symmetrically distinct ice configurations with lattice constants under 1.1 GPa at 8 K ($a$ = 6.166 Å, $c$ = 5.689 Å). The energies with lattice constants under 1.1 GPa and 225 K ($a$ = 6.181 Å, $c$ = 5.698 Å) are shown as solid circles, and the energies with lattice constants from the recovered sample ($a$ = 6.27 Å, $c$ = 5.79 Å) are shown as open diamonds. The nonsignificant role of the lattice constants on the relative energetics is evident by the fact that most of the points do not deviate much from the diagonal line. Under all three sets of lattice constants we considered, a ferroelectric structure shown in Figure 5 is found to be the ground state.

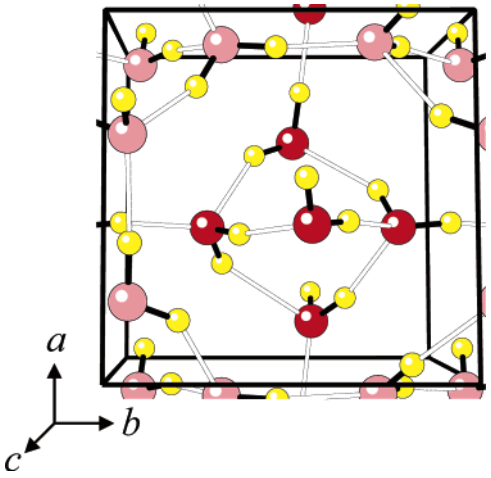


**Figure 5.** A candidate for the low-temperature proton-ordered form of ice-VI—the most stable structure as determined by DFT calculation on all 45 symmetrically distinct ice configurations permitted in the primary unit cell of ice-VI. Our ab intio calculations also confirm that its preferred stability is valid regardless the lattice constants used (see caption of Figure 4).

The temperature dependence of the heat capacity ($C_v$) and the average energy ($\langle E \rangle$), derived from the partition function, are shown in Figures 6a and 6b, respectively. Our calculations indicate a "phase transition temperature" at around 80 K, but we should note that this temperature is a very rough estimate because the "ensemble" used here is limited to those configurations in the primary unit cell. A more extensive sampling of the phase space (including ice configurations with more disordered H-bond networks in larger unit cells) is required and will be addressed in a forthcoming paper.

*Local Ordering of $O_1$.* Beside the long-range proton ordering as discussed above, it is also possible that the ordering is partial

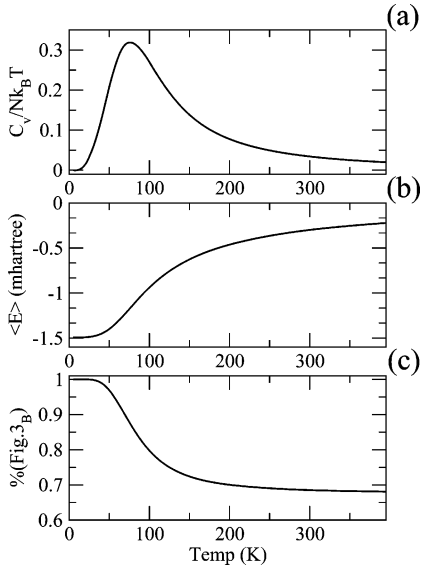


**Figure 6.** Temperature dependence of the various quantities: heat capacity (upper panel), potential energy (middle panel), and probability of orientation B (lower panel). The units of the energy are in mhartree, and the heat capacity is in reduced and dimensionless form. All three curves indicate a "phase transition" occurs at ~80 K.

and short-ranged as suggested by dielectric data.[20] The latter would not be reflected in the Bragg diffraction data and only be visible in diffuse scattering contributions, which are very difficult to measure at high pressure. In the following, we shall discuss one possible local ordering scheme that is unique in ice-VI, and we should also note that other local ordering schemes on a short-range scale are possible.

In a fully disordered structure every water molecule has six possible orientations. In the ice-VI structure a peculiarity arises in that for $O_1$ all neighboring H atoms belong to only one crystallographically distinct species, $H_2$ (Figures 2 and 3). Still, as a consequence of the tetragonal symmetry of the $O_1$ site, two crystallographically distinct water arrangements exist shown as parts A and B in Figure 3. In the time−space-averaged picture that is sampled by Bragg diffraction, no distinction can be made between a situation where all six configurations occur with equal probability of 1:6 and the other extreme, in which the four configurations of type B occur with a probability of 1:4 each and the two configurations of type A do not occur at all; all transitions between these two extremes can occur. This fact allows for a systematic partial water molecule ordering around the $O_1$ site without changing the space group symmetry of the crystal structure. In contrast, a systematic partial ordering on the $O_2$ site preferring one of the configurations cannot be achieved without a change of space group symmetry.

Theoretical calculations can fill the void, due to experimental limits explained above. In our theoretical framework, the temperature dependence on local ordering of $O_1$ can be derived from the approximated partition function ($Q_N$). For example, the probability for water molecules centered on $O_1$ to take orientation B (denoted as $P(B;T)$) can be calculated by $P(B;T) = \Sigma_i^M B(O_1) f_i \exp(-\beta E_i)/Q_N$, where

$$B(O_1) = \begin{cases} 1 & O_1 = B \\ 0 & O_1 = A \end{cases}$$

It is obvious that the probability for water molecules at $O_1$ to take orientation A (denoted as $P(A;T)$) is equal to $1 - P(B;T)$; thus only the temperature dependence of $P(B;T)$ is shown in Figure 6c. It is clear from Figure 6c that at low temperatures orientation B is preferred, which is in line with the fact that the ground-state structure (shown in Figure 5) has 100% orientation B. As the temperature increases, $P(B;T)$ drops rapidly at "phase transition" temperature, and in the high-temperature limit $P(B;T)$ approaches 2:3, indicating a true disorder case.

## 4. Conclusions

We have examined the structure of ice-VI by density functional methods, and the intrinsic disorder is investigated by studying all ice-rule-allowed ice configurations in its primary unit cell. We found a significant amount of static distortions, by averaging through 45 symmetrically distinct configurations that represent a total of 576 possible arrangements, and the isotropic average of the static distortions from first principles calculations is consistent with previous indirect experimental estimates.

The covalent bond $R$(OH) in ice-VI is found to be about 0.98 Å, which is consistent with previous experimental estimates. Together with previous studies on ice-Ih and ice-VII, we conclude that the $R$(OH) is not sensitive to the change of the neighboring H-bond arrangements. The molecular angle of water ($\angle$HOH), however, shows strong dependence on the molecular orientation. While the $\angle$HOH follow the trends of the $\angle$OOO to accommodate a reasonable H-bonding angle, we found the deviation of $\angle$HOH in ice-VI from its gas-phase value is smaller than previously assumed. It is also interesting to note that the $\angle$HOH in ice-VI is smaller than that of the isolated cage water hexamers; we think this reduction of $\angle$HOH in crystalline phases is likely due to the repulsive interaction between the water molecules in the two sublattices.

Different proton-ordering schemes in the literature were examined, and the possible roles of the different lattice constants in under-pressure and recovered sample were also investigated. In total we have considered three sets of lattice constants, and a ferroelectric structure (shown in Figure 5) is found to be the ground-state regardless of the change in lattice constants. Our estimated phase transition temperature is about 80 K; under such low temperature it is difficult for proton ordering to occur. Attempts have been made by Minceva-Sukarova et al.[43,44] and Handa et al.[45] using KOH-doped ice samples, but no convincing evidence has been seen so far. It may, however, be possible to promote the ordering by adding other dopants.

**Acknowledgment.** Computational resources provided by BIRC at Nangyang Technological University (NTU) and financial support from NTU (J.L.K.) and DFG grant Ku920/9 (W.F.K.) are gratefully acknowledged.

## References and Notes

(1) Hobbs, P. V. *Ice Physics*; Clarendon Press: Oxford, U. K., 1974.

(2) Petrenko, V. F.; Whitworth, R. W. *Physics of Ice*; Oxford University Press: New York, 1999.

(3) Kuhs, W. F.; Finney, J. L.; Vettier, C.; Bliss, D. V. *J. Chem. Phys.* **1984**, *81*, 3612.

(4) Loerting, T.; Salzman, C.; Kohl, I.; Meyer, E.; Hallbrucker, A. *Phys. Chem. Chem. Phys.* **2001**, *3*, 5355.

(5) Klotz, S.; Strassle, T.; Nelmes, R. J.; Loveday, J. S.; Hamel, G.; Rousse, G.; Canny, B.; Chervin, J. C.; Saitta, A. M. *Phys. Rev. Lett.* **2005**, *94*, 025506.

(6) Koza, M. M.; Geil, B.; Winkel, K.; Köhler, C.; Czeschka, F.; Scheuermann, M.; Schober, H.; Hansen, T. *Phys. Rev. Lett.* **2005**, *94*, 122506.

(7) Guthrie, M.; Tulk, C. A.; Benmore, C. J.; Klug, D. D. *Chem. Phys. Lett.* **2004**, *397*, 335.

(8) Lobban, C.; Finney, J. L.; Kuhs, W. F. *Nature* **1998**, *391*, 268.

(9) Klotz, S.; Hamel, G.; Loveday, J. S.; Nelmes, R. J.; Guthrie, M.; Soper, A. K. *Phys. Rev. Lett.* **2002**, *89*, 285502.

(10) Martonák, R.; Donadio, D.; Parrinello, M. *J. Chem. Phys.* **2005**, *122*, 134501.
(11) Martonák, R.; Donadio, D.; Parrinello, M. *Phys. Rev. Lett.* **2004**, *92*, 225702.
(12) Kamb, B. *Science* **1965**, *150*, 205.
(13) Kuhs, W. F.; Ahsbahs, H.; Londono, D.; Finney, J. L. *Physica B* **1989**, *156*, 684.
(14) Ahsbahs, H.; Dorwarth, R.; Kuhs, W. F.; Londono, J. D. *High Pressure Res.* **1990**, *5*, 807.
(15) Dorwarth, R. X-ray and neutron diffraction studies on ice VI single crystals at high pressure. Ph.D. Thesis, Universität (TH) Karlsruhe, 1993.
(16) Kuhs, W. F.; Bauer, F. C.; Hausmann, R.; Ahsbahs, H.; Dorwarth, R.; Hölzer, K. *High Pressure Res.* **1996**, *14*, 341.
(17) Kuhs, W. F. *Acta Crystallogr., Sect. A* **1992**, *48*, 80.
(18) Kuhs, W. F.; Lehmann, M. S. *J. Phys., Colloq.* **1987**, *48*, 3.
(19) Kamb, B. Crystallography of ice. In *Physics and Chemistry of Ice*; Whalley, E., Jones, S. J., Gold, L. W., Eds.; Royal Society of Canada: Ottawa, Canada, 1973; p 28.
(20) Johari, G. P.; Whalley, E. *J. Chem. Phys.* **1976**, *64*, 4484.
(21) Johari, G. P.; Whalley, E. *J. Chem. Phys.* **1979**, *70*, 2094.
(22) Londono, J. D.; Kuhs, W. F.; Finney, J. L. *J. Chem. Phys.* **1993**, *98*, 4878.
(23) Kuo, J. L.; Klein, M. L. *J. Phys. Chem. B* **2004**, *108*, 19634.
(24) Singer, S. J.; Kuo, J.-L.; Hirsch, T. K.; Knight, C.; Ojamäe, L.; Michael L. Klein. *Phys. Rev. Lett.* **2005**, *94*, 135701.
(25) Kuo, J. L.; Klein, M. L.; Kuhs, W. F. *J. Chem. Phys.* **2005**, *123*, 134505.
(26) Buch, V.; Sandler, P.; Sadlej, J. *J. Phys. Chem. B* **1998**, *102*, 8641.
(27) Pauling, L. *J. Am. Chem. Soc.* **1935**, *57*, 2680.
(28) Bernal, J. D.; Fowler, R. H. *J. Chem. Phys.* **1935**, *1*, 515.
(29) Kuo, J. L.; Coe, J. V.; Singer, S. J.; Band, Y. B.; Ojamae, L. *J. Chem. Phys.* **2001**, *114*, 2527.
(30) Kuo, J. L.; Singer, S. J. *Phys. Rev. E* **2003**, *67*, 016114.
(31) Car, R.; Parrinello, M. *Phys. Rev. Lett.* **1987**, *62*, 403.
(32) Becke, A. D. *Phys. Rev. A* **1988**, *38*, 3098.
(33) Lee, C.; Yang, W.; Parr, R. G. *Phys. Rev. B* **1988**, *37*, 785.
(34) Troullier, N.; Martins, J. L. *Phys. Rev. B* **1991**, *43*, 1993.
(35) Benoit, M.; Romero, A. H.; Marx, D. *Phys. Rev. Lett.* **2002**, *89*, 145501.
(36) Chen, B.; Ivanov, I.; Klein, M. L.; Parrinello, M. *Phys. Rev. Lett.* **2003**, *91*, 215503.
(37) Silvestrelli, P. L.; Parrinello, M. *Phys. Rev. Lett.* **1999**, *82*, 3308.
(38) Kuhs, W. F.; Lehmann, M. S. The structure of ice-Ih. In *Water Science Reviews*; Franks, F., Ed.; Cambridge University Press: New York, 1986; Vol. 2; p 1.
(39) Kuhs, W. F.; Lehmann, M. S. In *Colston Symposium on Water and Aqueous Solutions*; Neilson, G. W., Ed.; Bristol, 1985.
(40) Tissandier, M. D.; Singer, S. J.; Coe, J. V. *J. Chem. Phys.* **2000**, *104*, 752.
(41) Koch, W.; Holthausen, M. *A Chemist's Guide to Density Functional Theory*, 2nd ed.; Wiley-VCH: Weinheim, Germany, 2001.
(42) Sukarova, B. The Raman spectra of high pressure forms of ice in their region of stability. Ph.D. Thesis, King's College, University of London, 1982.
(43) Minceva-Sukarova, B.; Slark, G.; Sherman, W. F. *J. Mol. Struct.* **1986**, *143*, 87.
(44) Minceva-Sukarova, B.; Slark, G.; Sherman, W. F. *J. Mol. Struct.* **1988**, *175*, 289.
(45) Handa, Y. P.; Klug, D. D.; Whalley, E. *J. Phys. Colloq.* **1987**, *48*, 435.